Geoderma 308 (2017) 36–45

Contents lists available at ScienceDirect

Geoderma

journal homepage: www.elsevier.com/locate/geoderma

An improved method for calculating slope length (λ) and the LS parameters of the Revised Universal Soil Loss Equation for large watersheds

Hongming Zhang[a], Jicheng Wei[a,*], Qinke Yang[b,*], Jantiene E.M. Baartman[c], Lingtong Gai[a,c], Xiaomei Yang[a,c], ShuQin Li[a], Jiantao Yu[a], Coen J. Ritsema[c], Violette Geissen[c]

[a] College of Information Engineering, Northwest A & F University, Yangling, Shaanxi 712100, China
[b] Department of Urbanology and Resource Science, Northwest University, Xi'an, Shaanxi 710069, China
[c] Soil Physics and Land Management Group, Wageningen University, Droevendaalsesteeg 4, 6708 PB Wageningen, The Netherlands

ARTICLE INFO

Handling Editor: Morgan Cristine L.S.

Keywords:
Soil erosion
RUSLE
LS
GIS
Terrain analysis

ABSTRACT

The Universal Soil Loss Equation (USLE) and its revised version (RUSLE) are often used to estimate soil erosion at regional landscape scales. USLE/RUSLE contain parameters for slope length factor (L) and slope steepness factor (S), usually combined as LS. However a major limitation is the difficulty in extracting the LS factor. Methods to estimate LS based on geographic information systems have been developed in the last two decades. L can be calculated for large watersheds using the unit contributing area (UCA) or the slope length (λ) as input parameters. Due to the absence of an estimation of slope length, the UCA method is insufficiently accurate. Improvement of the spatial accuracy of slope length and LS factor is still necessary for estimating soil erosion. The purpose of this study was to develop an improved method to estimate the slope length and LS factor. We combined the algorithm for multiple-flow direction (MFD) used in the UCA method with the LS-TOOL (LS-TOOL$_{SFD}$) algorithms, taking into account the calculation errors and cutoff conditions for distance, to obtain slope length (λ) and the LS factor. The new method, LS-TOOL$_{MFD}$, was applied and validated in a catchment with complexly variable slopes. The slope length and LS calculated by LS-TOOL$_{MFD}$ both agreed better with field data than with the calculations using the LS-TOOL$_{SFD}$ and UCA methods, respectively. We then integrated the LS-TOOL$_{MFD}$ algorithm into LS-TOOL developed in Microsoft's .NET environment using C# with a user-friendly interface. The method can automatically calculate slope length, slope steepness, L, S, and LS factor, providing the results as ASCII files that can be easily used in GIS software and erosion models. This study is an important step forward in conducting accurate large-scale erosion evaluation.

1. Introduction

Large-scale soil erosion is a severe problem affecting the development of China, particularly on the Loess Plateau. The Chinese Soil Loss Equation (CSLE) (Liu et al., 2002), which was derived from the Universal Soil Loss Equation (USLE) (Wischmeier and Smith, 1978) and the subsequent revised USLE (RUSLE) (Renard et al., 1997), was used to estimate soil erosion in China at the scale of regional landscapes (Yao et al., 2012). USLE/RUSLE and CSLE are often used to estimate soil erosion for large areas, up to country level (Yang et al., 2013). The USLE/RUSLE/CSLE equation computes the average annual soil erosion by multiplying several factors together, which includes: rainfall (R) factor (MJ mm ha^{-1} h^{-1} y^{-1}); soil erodibility (K) factor (Mg h^{-1} MJ^{-1} mm^{-1}); slope length and steepness (LS) factor; cover management factor (C) and support practice factors (P). L, S, C, and P are dimensionless. The details of these parameters and their effects on erosion prediction are discussed in Renard et al. (1991, 1997).

L and S in the equation are generally combined as LS, representing the effect of the topography on erosion rates (Van Remortel et al., 2004). The equations for calculating LS in the RUSLE are:

$$LS = L \cdot S \quad (1)$$

$$L = (\lambda/22.13)^m \quad (2)$$

$$m = \beta/(1+\beta) \quad (3)$$

$$\beta = (\sin\theta)/[3\cdot(\sin\theta)^{0.8} + 0.56] \quad (4)$$

$$\begin{aligned} S &= 10.8\cdot\sin\theta + 0.03 \quad \theta < 9\% \\ S &= 16.8\cdot\sin\theta - 0.5 \quad \theta \geq 9\% \end{aligned} \quad (5)$$

where λ is the slope length (m), m is a variable length-slope exponent, β is a factor that varies with slope gradient, and θ is the slope angle.

* Corresponding authors.
E-mail addresses: zhm@nwsuaf.edu.cn (H. Zhang), weijc@nwsuaf.edu.cn (J. Wei), qkyang@nwu.edu.cn (Q. Yang).

http://dx.doi.org/10.1016/j.geoderma.2017.08.006
Received 12 December 2016; Received in revised form 17 July 2017; Accepted 4 August 2017
Available online 30 August 2017

Slope length (λ) in this equation has been defined as "the distance from the point of origin of overland flow to either of the following, whichever is limiting for the major part of the area under consideration: (a) the point where the slope decreases to the extent that deposition begins, or (b) the point where runoff enters a well-defined channel that may be part of a drainage network or a constructed channel such as a terrace or diversion" (Wischmeier and Smith, 1978).

USLE and RUSLE were originally developed for gently sloping cropland and the topography factor (LS) was one dimension. When applying USLE or RUSLE equation to calculate the average annual sheet and rill erosion per unit area at watershed or even larger scales, however, topography becomes two-dimensional and LS is more difficult to estimate than other terms in the equation (Ligonja and Shrestha, 2015; Van Remortel et al., 2004). Procedures have been developed in the last 20 years that allow the use of geographic information systems (GISs) to generate both USLE- and RUSLE-based validated algorithms used to calculate LS.

Moore and Wilson (1992) presented a simplified equation using unit contributing area (UCA) to calculate LS for three-dimensional terrain:

$$LS = \left(\frac{A_s}{22.13}\right)^m \left(\frac{\sin(\theta)}{0.0896}\right)^n, \tag{6}$$

where A_s is the unit contributing area (m), θ is the slope in radians, and m (0.4–0.56) and n (1.2–1.3) are exponents.

Desmet and Govers (1996) used the algorithm for multiple-flow direction (MFD) developed by Quinn et al. (1991) to calculate contributing areas and then LS in cells of data for digital elevation models (DEMs). Winchell et al. (2008) and Rodriguez and Suarez (2012) improved this method by comparing several variations of the GIS approach. A new European topographical factor was extracted using the UCA method (Panagos et al., 2015). The advantage of the UCA method to replace the slope length, as proposed in all these methods, is its ease of calculation. However, RUSLE/USLE cannot be used to China directly because China has more steep slopes (> 10°). Therefore, CSLE was developed taking into consideration the Chinese soil environment (including the modified equation that can calculate LS factor in > 10° conditions). Thus the UCA method which was designed for RUSLE/USLE cannot be used directly for CSLE. In CSLE, the calculation of L is based on the slope length:

$$\begin{aligned} &L = (\lambda/22.1)^m \\ &m = 0.2 \quad \theta \le 1.7\% \\ &m = 0.3 \quad 1.7\% < \theta \le 5.2\% \\ &m = 0.4 \quad 5.2\%^\circ < \theta \le 9\% \\ &m = 0.5 \quad \theta > 9\% \end{aligned} \tag{7}$$

where λ is the slope length (m), m is a variable slope-length exponent, and θ is the slope angle (°). S is calculated based on slope steepness, including the steep slopes occurring on the Loess Plateau of China.

$$S = \begin{cases} 10.8\sin\theta + 0.03 & \theta < 9\% \\ 16.8\sin\theta - 0.05 & 9\% \le \theta < 17.6\% \\ 21.9\sin\theta - 0.96 & \theta \ge 17.6\% \end{cases} \tag{8}$$

Slope length is also needed to predict zones of soil deposition (Winchell et al., 2008). A valid method for calculating slope length would thus be a good way to apply the CSLE to the Loess Plateau.

Dunn and Hickey (1998), Hickey (2000), Van Remortel et al. (2001, 2004), and developed new models for identifying breaks in slope length involving changes in the slope turning point and channels based on the definition of slope length (Wischmeier and Smith, 1978). These methods can overcome some of the disadvantages of the UCA method (Galdino et al., 2016), such as not considering channels. These methods, however, use algorithms for single flow direction (SFD) (O'Callaghan and Mark, 1984) to calculate slope length, which allows only parallel and convergent flows and produces biased results when using DEMs (Orlandini et al., 2014). Moore and Burch (1986a, 1986b) recognised that higher rates of erosion or deposition occurred at the convergence of a catchment, as also postulated in USLE/RUSLE/CSLE. These results have implied that sheet flow had the lowest sediment transport capacity and that the topographic convergence or divergence in a catchment could increase or decrease the unit stream power and the capacity of sediment transport. MFD algorithms can accommodate convergent and divergent flow and perform better than SFD algorithms for real terrains (Orlandini et al., 2012; Wilson et al., 2007). The UCA method therefore uses an MFD algorithm to estimate LS. However, the UCA method has not been used to calculate the slope length, taking into consideration the cutoff conditions. Therefore, improvement of the spatial accuracy of slope length and LS factor is still necessary for estimating soil erosion (Feng et al., 2016).

The aim of this paper is to propose an improved algorithm that combine the advantage of UCA method and the LS-TOOL$_{SFD}$ method. A GIS-based method for calculating λ and slope steepness were developed. The calculated slope length and steepness were then entered into a newly developed algorithm to calculate LS, taking the cutoff position for slope change and channel network into consideration and using the MFD algorithm. The new method, LS-TOOL$_{MFD}$, was applied to the Xiannangou catchment in China. The calculated slope length and LS were compared with those calculated using the UCA method, LS-TOOL$_{SFD}$, and field data. This algorithm can save computing time and improve the accuracy of large scale erosion modeling.

2. Materials and methods

2.1. Cell-based slope length calculation

The calculation algorithm for slope length and flow convergence as developed by Van Remortel et al. (2004), was revised by Zhang et al. (2013). The equation to calculate the slope length is:

$$\lambda_{i,j} = \frac{A_{i,j-out}}{D_{i,j}}, \tag{9}$$

where $A_{i,j-out}$ is the contributing area at the outlet of grid cell with coordinates (i,j) (m^2), $D_{i,j}$ is the effective contour length of coordinates (i,j) (m), and $\lambda_{i,j}$ is the slope length of coordinates (i,j) (m).

In differential form:

$$\lambda_{i,j} = \int_{i_0,j_0}^{i,j} \lambda(t)dt. \tag{10}$$

A cell is the basic calculation unit for raster data, and slope length can be defined as accumulating each cell's slope length (CSL) along a flow path from its start point (i_0, j_0) to its end point (i,j):

$$\lambda_{i,j} = \int_{i_0}^{i} \int_{j_0}^{j} \mathrm{CSL}_{i,j} didj \tag{11}$$

We revised the equations by Zhang et al. (2013).CSL will be determined by slope aspect when the MFD algorithm is used, because different aspect means a different length of the current cell.

The algorithm for a third-order finite difference (3FD) (Wood, 1996) was used to calculate slope aspect and gradient because it is the least sensitive to the DEM data error (Zhou and Liu, 2004). The calculation of CSL and slope length using the MFD algorithm is described in the next section.

2.2. LS-TOOL$_{MFD}$: LS calculation

Our methodology to calculate the slope length, slope steepness, L and S is illustrated in Fig. 2:

Step 1: Input DEM data (an ASCII file with header information).

Step 2: Analyse the DEM data to look for sinks. If an isolated cluster of sinks (> 5 cells) is encountered, the calculation will stop, otherwise the following steps will be executed.

Step 3: Fill any spurious (i.e. no data and sink) single cells within

the source DEM using an routine iterative method (Van Remortel et al., 2004).

Step 4: Use the 3FD algorithm (Wood, 1996) to estimate the slope angle and aspect.

Step 5: Calculate cell downhill-flow direction (outflow proportion) and cutoff point for each direction using the MFD algorithm.

Step 6: Calculate CSL using the slope aspect.

Step 7: Use a forward-and-reverse traversal method to calculate the contributing area of each cell.

Step 8: Calculate slope length using the data for the outflow proportion, cell slope length, and contributing-area threshold.

Step 9: Determine L using the slope length and the slope-length exponent.

Step 10: Calculate S using the slope angle.

Step 11: Calculate LS.

We focused on the calculation of slope length and LS (steps 4–8), which are described in detail below.

2.3. Estimation of slope angle and aspect

After the depressionless DEM data have been produced, the slope angle (θ) and aspect (A) of the cell in the downhill direction is calculated by the 3FD algorithm (Wood, 1996):

$$\theta = \arctan\sqrt{f_x^2 + f_y^2} \tag{12}$$

$$A = 270° + \arctan\left(\frac{f_y}{f_x}\right) - 90°\frac{f_x}{|f_x|} \quad (f_x \neq 0) \tag{13}$$

The computational algorithms to calculate f_x and f_y in Eqs. (12) and (13) are:

$$f_x = (z_5 - z_7 + z_4 - z_8 + z_3 - z_1)/6d \tag{14}$$

$$f_y = (z_1 - z_7 + z_2 - z_6 + z_3 - z_5)/6d \tag{15}$$

where z_1 to z_9 are the elevations of cells 1 to 9 (Fig. 3a), d is the grid cell size, and f_x and f_y are the gradients in the W-E and N-S directions.

2.4. Calculation of outflow direction

The MFD algorithm assigns the outflow proportion for each downslope direction. The calculation and the relative amount are then calculated as (Quinn et al., 1991):

$$\Delta P_i = \frac{\tan\theta_i L_i}{\sum_{j=1}^{n} \tan\theta_j L_j} \tag{16}$$

where ΔP_i is the amount (proportion) passed onto the ith downhill cell, n is the total number of downhill directions (max. 8), i is one of the eight cells surrounding the current cell, L_i is either the cardinal ($0.5 * \text{grid size}$) or diagonal ($0.354 * \text{grid size}$) contour length of the ith direction, and θ_i is the gradient in the ith downhill direction.

The termination of a slope length was determined by the two conditions defining the slope length: the slope cutoff point and the channel network. The MFD algorithm divides the flow out of a cell over several receiving cells, so the cutoff points were saved in memory as cutoff directions (Fig. 3b). The outflow proportion should be expressed by considering the cutoff point. For our purposes, the cutoff point where the sediment will be deposited was defined by the gradient from the central cell to the eight surrounding cells. For example, if the elevation was higher in the central cell than any of the eight surrounding cells and the change of slope angle between the central cell and the surrounding cells was > 50% (slope decreasing by > 50%), then the cell in this direction was the cutoff point, and the next cell could not accumulate the slope length from the current direction. We used the elementary cutoff conditions in Fig. 1 to calculate the slope length and thus made the following assumptions for the USLE/RUSLE equation (Griffin et al., 1988; Wilson, 1986): 1) for slopes > 5%, the turning point (P1, Fig. 1) is when the change in gradient is > 70%, 2) for slopes < 5%, the turning point is when the change in gradient is > 50%, or 3) the turning point is when a channel network is encountered (P2, Fig. 1).

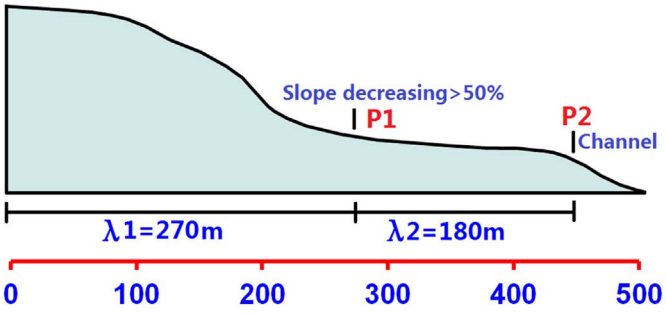

Fig. 1. Slope length for USLE/RUSLE/CSLE. λ1 is the distance from the point of origin of overland flow to point P1 where the slope decreases to the extent that deposition begins, and λ2 is the distance from the cutoff point (P1) (which is also a new start point of a new slope length due to deposition) to where runoff enters a channel (P2).

The data points of the flow proportion for each direction are created as calculated by the algorithm and saved as a floating-point format matrix. Since ΔP_i is always a positive value, in order to differentiate the cutoff point direction from other directions, the programme will save ΔP_i as $-\Delta P_i$ in the matrix if direction i is the cutoff point direction. (Fig. 3b) This proportion does not accumulate to the next cell in this direction, so every point of the matrix has eight values representing the eight directions.

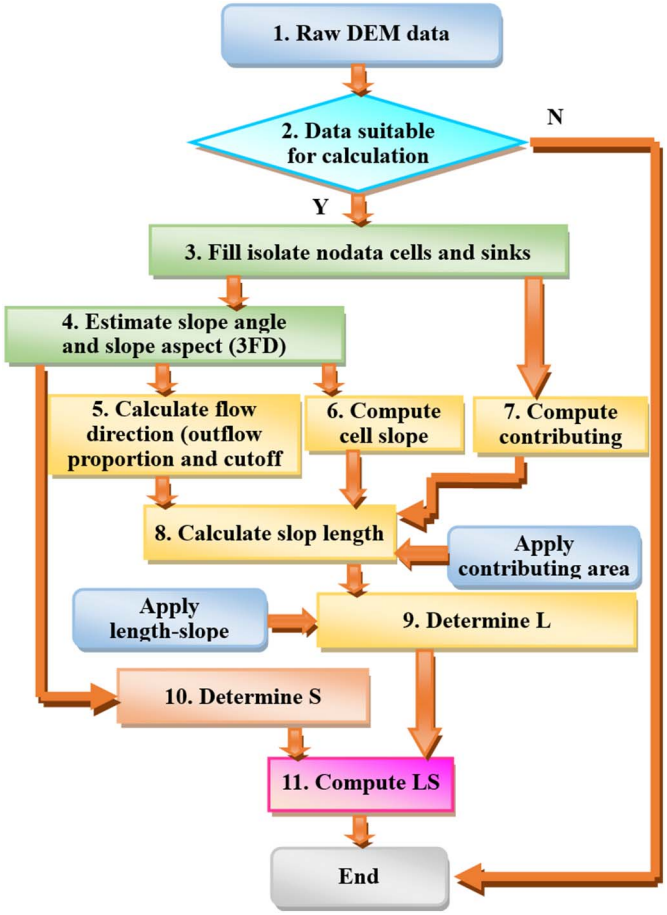

Fig. 2. Flowchart of the procedure for calculating slope length, slope steepness, L, S, and LS in the algorithm of this paper.

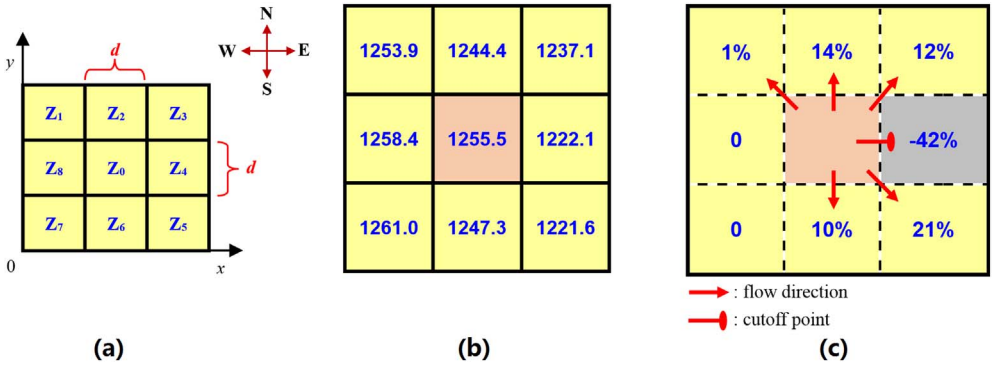

Fig. 3. Cell code, outflow proportion and cutoff directions from the DEM. (a) The cell code for a 3 × 3 window used in Eqs. (15) and (16). (b) 3 × 3 DEM data (elevations (m)) were used to calculate outflow proportions and cutoff directions. (c) The outflow proportions in eight directions; 0 indicates no flow proportion, the negative number represents the cutoff direction, and the sum of the proportion was 100% for each grid.

2.5. Calculation of cell slope length (CSL)

CSL is the distance from the cell itself to the next cell along the flow direction. Distance over raster DEMs are normally calculated step-by-step accumulating Euclidean distances, which depends on the size of the cells and on the direction of travel between cells. This is not always the actual length. As has been pointed out, this standard way of calculating length or distance leads to errors, because the distance are correct only at angles that are multiple of 45°, even when using a high-resolution raster (da Paz et al., 2008; de Smith, 2004). This was called distance transforms error. In a previous study, Zhang et al. (2013) showed that LS-TOOL$_{SFD}$ estimated slope lengths to be slightly longer than slope length as measured in the field in some locations. In the present study, we used the values of the distance transforms used by da Paz et al. (2008) to reduce errors, which are almost 0.962 times the CSL. The size of the cells was thus calculated using:

$$CSL = 0.5*d \quad \text{if slope steepness } (\theta) \text{ is 0, or} \tag{17}$$

$$CSL = d*a*(|\sin A| + |\cos A|) \quad \text{if } \theta \text{ is not 0} \tag{18}$$

where a is 0.962 (da Paz et al., 2008), A is the slope aspect (°), and d is the cell size (m).

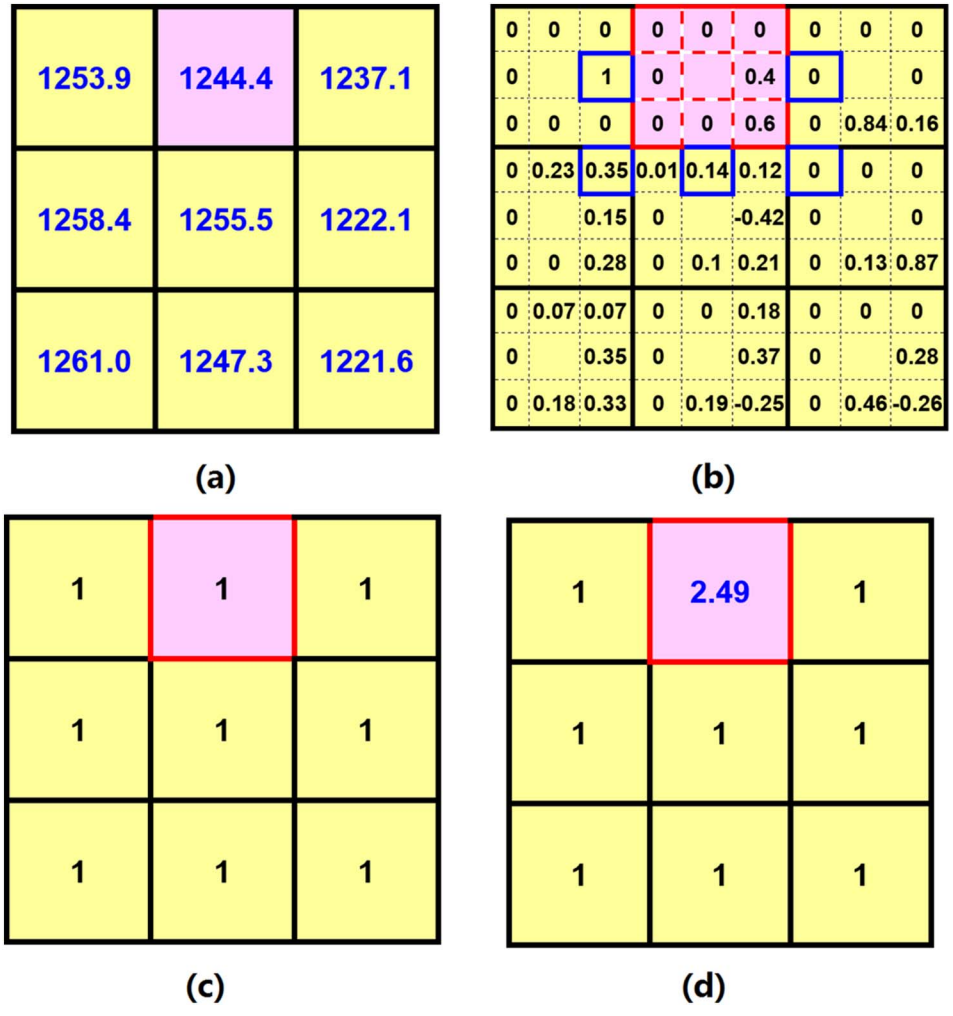

Fig. 4. Calculation of the contributing area. (a) The original DEM elevations in metres. (b) The outflow proportion of each cell in the eight directions (blue border cells are the portion of the surrounding cells added to the red border cell depending on the portion). (c) The initial contributing area. (d) The contributing area of the second cell in the calculation using the DEM data. The data for outflow proportion and initial contributing area are shown in the red box:

2.49 = 1 + 1 × 1 + 1 × 0.35 + 1 × 0.14 + 1 × 0 + 1 × 0. (For interpretation of the references to colour in this figure legend, the reader is referred to the web version of this article.)

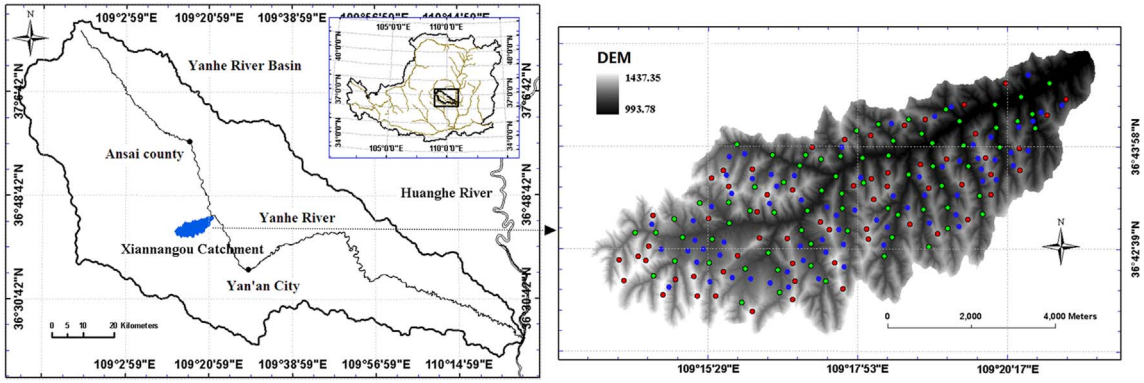

Fig. 5. (a) The main map shows the location of the Xiannangou catchment (light green shading) on the Loess Plateau in the middle reaches of the Yellow River Basin. The inset map shows the location of the Loess Plateau in China. (b) The map shows the 5-m DEM of the study site. Red dots are mainly hilltops, ridges, or local high points; green dots are channels, gullies, or roads; and blue dots are gently rolling areas. (For interpretation of the references to colour in this figure legend, the reader is referred to the web version of this article.)

2.6. Calculation of accumulated area

Calculating the accumulated area using the matrix for the outflow proportion is the first step for extracting channels. Tarboton et al. (1991) suggested that channels could be identified by calculating the accumulated-area array matrix and defining channels as pixels exceeding a threshold of accumulated area. If the accumulated area of a cell in the direction of the outflow of the current cell is larger than the threshold, the cell should be part of a channel network, and the accumulation of slope length is then terminated.

The calculation of the accumulated area was an iterative procedure calculated by an algorithm for forward-and-reverse traversal accumulation using the initial accumulated-area (Fig. 4c) and outflow-direction matrices (Fig. 4b):

(1) The accumulated-area matrix is created with an initial value of 1 assigned to all cells in the matrix except those with no data (Fig. 4c).
(2) Using a forward traversal method beginning with the upper left cell moving cell by cell to the lower right cell of the array matrix (left to right and top to bottom), sum the accumulated area value of the surrounding eight cells (accumulated area value multiply corresponding absolution value of outflow portion values if it's not zero) which flow into the current cell. If the sum value plus the initial accumulated area matrix is greater than the current value then new value replaces the current cell value. In this way, the forward direction traverse (i.e., from the upper left to the lower right) accumulates all possible flowpath cells flowing to the east, southeast and south directions (Fig. 4d).
(3) A reverse traversal method is applied from the lower right to the upper left. The process is the same as the forward method; a smaller value must be replaced with a larger value.

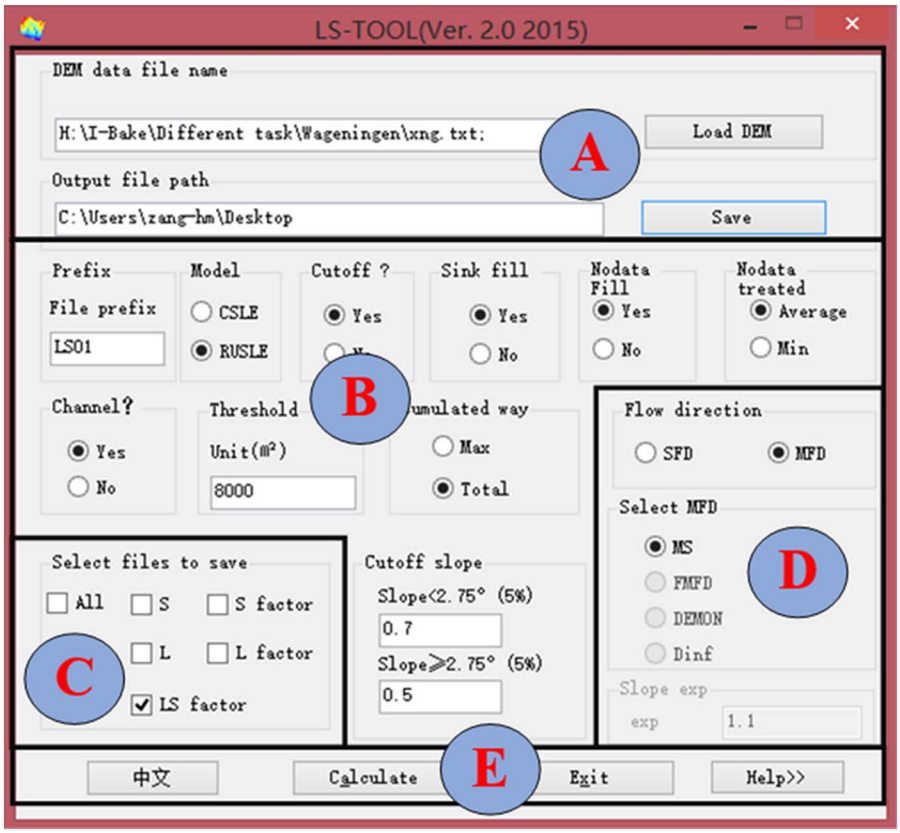

Fig. 6. The GUI of LS_TOOL. The section denoted by A, B, C, D, and E are as described in the text.

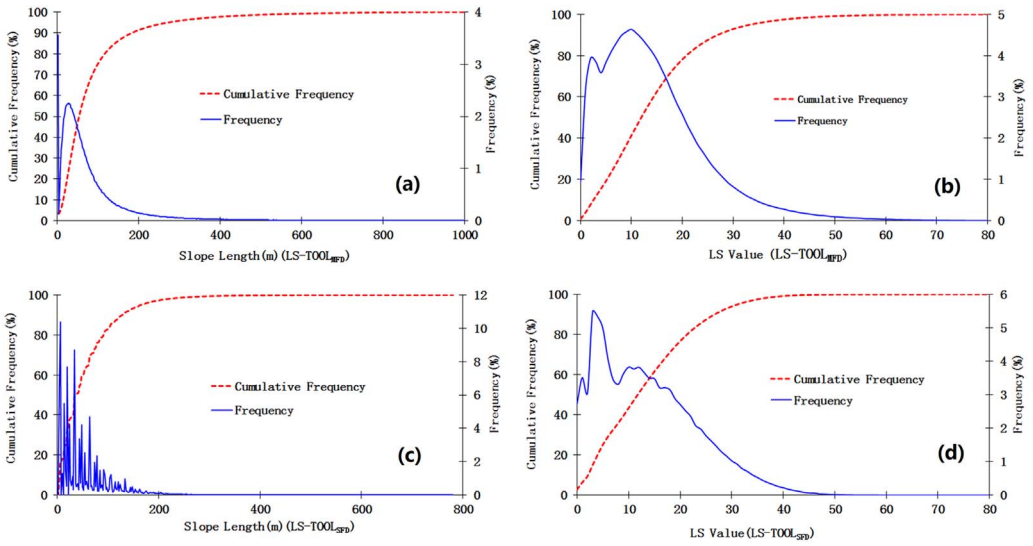

Fig. 7. Frequency and cumulative-frequency curves for slope length (a, c) and LS (b, d) produced by LS-TOOL$_{MFD}$ (a, b) and LS-TOOL$_{SFD}$ (c, d) for the study area.

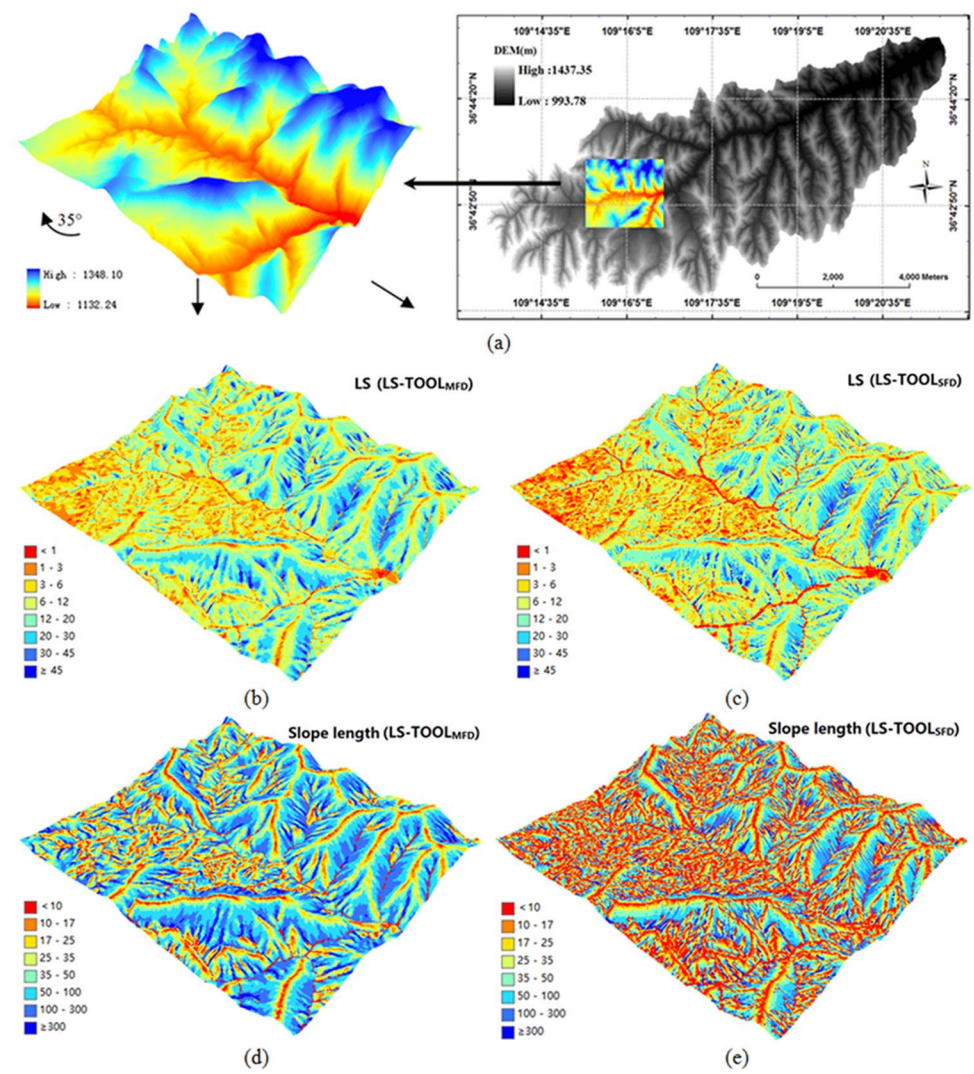

Fig. 8. Spatial distribution of slope length and LS calculated using LS-TOOL$_{SFD}$ and LS-TOOL$_{MFD}$. (a) The 5-m DEM data for the Xiannangou catchment (right map) with details for a subset of the data (left map). (b) Test run for slope length using LS-TOOL$_{MFD}$ (mean, 66.13; SD, 67.34). (c) Test run for LS using LS-Tool$_{MFD}$ (mean, 11.97; SD, 8.93). (d) Test run for slope length using LS-TOOL$_{SFD}$ (mean, 61.69; SD, 65.66). (e) Test run for LS using LS-Tool$_{SFD}$ (mean, 8.94; SD, 8.56).

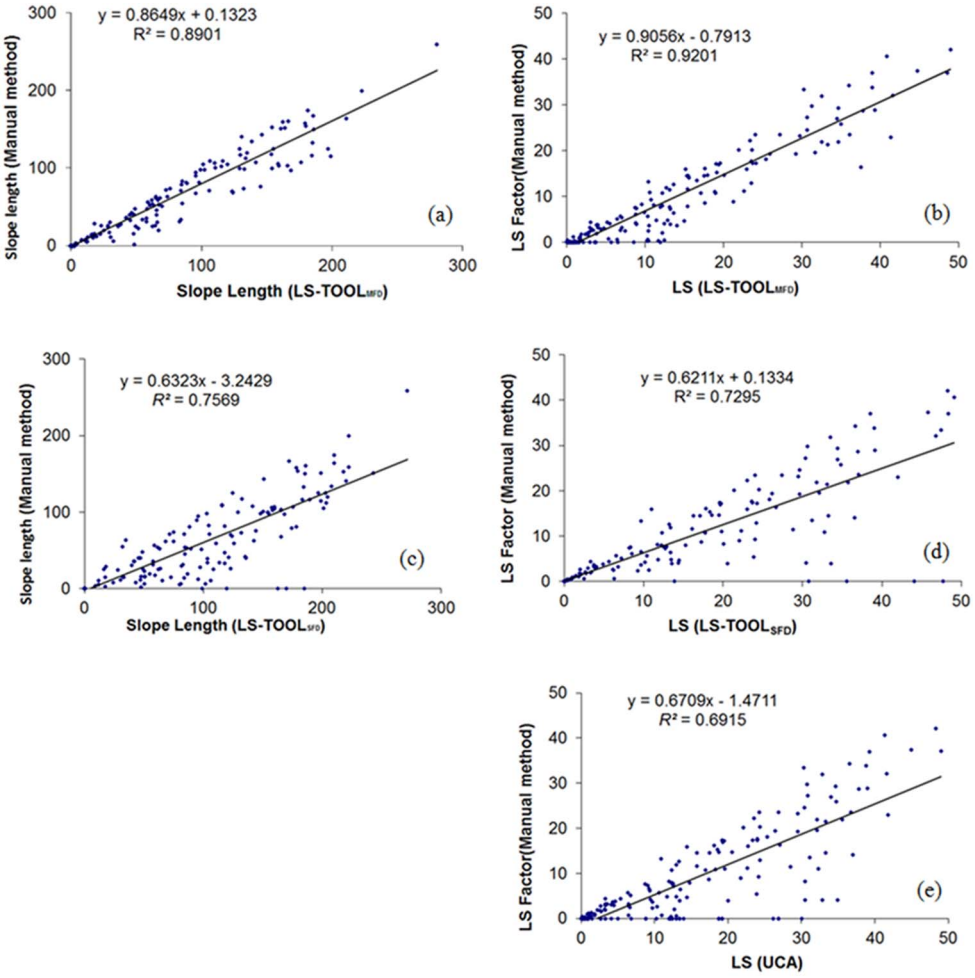

Fig. 9. Linear-regression relationship of slope length (a, c) and LS (b, d, e) for the field data with LS-TOOL$_{MFD}$, LS-TOOL$_{SFD}$, and the UCA method.

(4) The forward-and-reverse traversal method is run iteratively until the accumulated area in any cell no longer changes.

2.7. Accumulated slope length

Slope length can be calculated using the data for CSL, outflow proportion, and accumulated area. Calculating accumulation is similar to the previous section. Calculating the slope length, however, requires that the outflow proportion for the surrounding eight cells is > 0 and that the accumulated area of these cells is smaller than the threshold. The slope length of the current cell is the CSL of the cell summed with the current values multiplied by the outflow proportions for all eight surrounding cells.

2.8. Determination of L, S, and LS

S factor and L factor can now be calculated. We used the equations by (McCool et al., 1997) for calculating the RUSLE LS and the equations by Liu et al. (2002) for calculating the CSLE LS. The LS-TOOL algorithm was integrated as a tool which can automatically calculate slope length, slope steepness, L factor, S factor, and LS factors, providing the results as ASCII files which can be easily used in some GIS software.

2.9. Comparison of slope length and LS estimated by different methods with field data

We applied our method in the Xiannangou catchment (44.85 km^2) on the northwestern Loess Plateau, Shaanxi Province, China (Fig. 5), centred at 36.72°N, 109.30°E. We used a hydrologically correct DEM (Hc-DEM) data set (Yang et al., 2007) with a grid size of 5 m per pixel. A Hc-DEM is a depressionless DEM of good quality which can be developed using topographic and hydrographic data from topographic maps with TOPOGRID in ARC/INFO or ANUDEM (Liu et al., 2002; Zhang et al., 2017).

We compared slope length and LS calculated by LS-TOOL$_{MFD}$ with those collected from field work following the field instructions for sampling suggested by (McCool et al., 1997) and (Griffin et al., 1988). Obtaining slope lengths and gradients for the entire catchment was difficult, actually, an infinite number of slope lengths exist in the field so some particular position on the landscape were chosen as the location for a slope length. We selected a subset of 200 sample locations (Fig. 5b). Red dots are mainly hilltops, ridges, or local high points; green dots are channels, gully, or roads. For the gently rolling areas (Blue points), we walked upslope from the local high points, moving perpendicular to the contour, until the origin of overland flow is reached. In order to avoid the errors of field data, 85% slopes are short slope (length < 100 m).

The three GIS methods (UCA, LS-TOOL$_{SFD}$, and LS-TOOL$_{MFD}$) were compared by calculating slope length and LS using each method. To find a reasonable value for the accumulation threshold for the DEM used, 25 channel head points were labelled on the Google image of the study area and multiple accumulation thresholds were tested. Finally, we selected a threshold of accumulated area of 4000 m^2 for LS-TOOL$_{MFD}$, because this threshold corresponded well to the real channels.

With the UCA, because there is a threshold of the slope length which usually does not exceed 1000 ft (304.8 m) (Renard et al., 1997). We chose to use Eq. (6) ($m = 0.4$, $n = 1.3$) following Jabbar's (2003)

Table 1
RMSEs of the slope length and LS calculated by all three methods.

Method	Slope length	LS
LS-TOOL$_{MFD}$	24.24	4.27
LS-TOOL$_{SFD}$	48.51	8.86
UCA	–	9.33

approach, with a maximum accumulation of 60 grid cells using the spatial analyst tools in ArcGIS.

The LS-TOOL$_{SFD}$ method was implemented using C# program (Zhang et al., 2013).

The graphical user interface (GUI) of LS-TOOL$_{MFD}$ is shown in Fig. 6. To use and compare the difference of the two methods (LS-TOOL$_{SFD}$ and LS-TOOL$_{MFD}$), we integrated the LS-TOOL$_{MFD}$ algorithm into LS-TOOL developed by Microsoft's .NET environment using C# with a user-friendly interface (Zhang et al., 2013). The user interface is thus similar to that of LS-TOOL$_{SFD}$, but the algorithm is completely different. The five sections most relevant for the calculation of LS are denoted in red from A to E. Their functionality is described by Zhang et al. (2013). The only different section is D: radio button 'MFD' should be selected for calculating slope length, slope steepness, S, L, and LS using our MFD algorithm. The other methods indicated in section D of Fig. 6 (FMFD, Dinf and DEMON) are not available at the moment, they will be finished in ongoing further research.

The accuracy of slope length and LS calculated using the various algorithms were evaluated by determining the linear-regression relationship and the root mean square error (RMSE) of the residuals:

$$\mathrm{RMSE} = \sqrt{\frac{\sum_{i=1}^{n} (L_i - l_i)^2}{n}} \quad (19)$$

where n is the number of studied grid cells, L_i is the calculated slope length or LS at grid cell i, and l_i is the reference slope length or LS from the corresponding grid cell calculated with the DEM of the Xiannangou catchment (Fig. 5).

3. Results

3.1. Comparing slope length and LS calculated by the different methods

Frequency and cumulative-frequency curves for slope length and LS calculated by LS-TOOL$_{SFD}$ and LS-TOOL$_{MFD}$ are shown in Fig. 7.

Slope lengths calculated using LS-TOOL$_{MFD}$ were normally distributed, with 67.4% of the slope lengths < 80 m, 81.5% < 120 m, and 95.2% < 300 m (Fig. 7a). The LS values were also normally distributed, with 99.4% < 72, 88.2% < 30, and 53.2% between 7 and 22 (Fig. 7b). These LS results agreed well with those reported by McCool et al. (1997).

Slope length and LS calculated using LS-TOOL$_{SFD}$ are shown in Fig. 7c and d, with 68.3% of the slope lengths < 80 m, 81.8% < 120 m, and 95.6% < 300 m, and with 99.5% of the LS values were < 72, 88.3% < 30, and 54.3% between 7 and 22. The cumulative frequency was thus lower using LS-TOOL$_{MFD}$ than LS-TOOL$_{SFD}$ for the same slope length.

LS-TOOL$_{MFD}$ produced a smoother and more gently increasing frequency curve for slope length than LS-TOOL$_{SFD}$. Under the influence of slope length, the frequency curve for LS calculated by LS-TOOL$_{SFD}$ increased abruptly near a value of 5 (Fig. 7d).

3.2. Comparing spatial distribution of slope length and LS estimated by the different methods

The spatial distribution of the slope lengths calculated by the two methods is shown in Fig. 8. For clarity, we used a subset of the DEM data (Fig. 8a).

The slope length and LS obtained by LS-TOOL$_{MFD}$ spatial distributions were smoother (Fig. 8b, d) than the LS-TOOL$_{SFD}$ distributions (Fig. 8c, e). This indicated less abrupt variations in the magnitude of slope length and LS factor for adjacent cells. LS-TOOL$_{MFD}$ produced a longer mean slope length (> 4.44 m) than LS-TOOL$_{SFD}$ (Fig. 8d). Under the influence of slope length, LS-TOOL$_{MFD}$ also produced a higher LS (> 3.03) than LS-TOOL$_{SFD}$.

The performance of LS-TOOL$_{MFD}$ varied in different parts of the landscape (Fig. 8d). Shorter slope lengths were distributed at the ridges, rills, and channels. Slope lengths increased smoothly in the downhill direction. Convergence and divergence could be accommodated. The shorter slope lengths calculated using LS-TOOL$_{SFD}$ (Fig. 8e) were also distributed on the ridges and in the channels, but the slope lengths increased discontinuously along the hillslopes, which did not correspond well with the real terrain.

3.3. Comparison with field data

We compared slope length and LS calculated by the UCA method, LS-TOOL$_{MFD}$, and the field data. The UCA method could only calculate LS, so we only compared the LS values from the LS-TOOL$_{MFD}$ and field data.

LS-TOOL$_{MFD}$ calculated slope length better than LS-TOOL$_{SFD}$ when compared to the results from the field data (Fig. 9a, c). LS-TOOL$_{MFD}$ also calculated LS better than LS-TOOL$_{SFD}$ and the UCA method. (Fig. 9b, d, and e).

The RMSEs of the slope length and LS calculated by LS-TOOL$_{MFD}$, LS-TOOL$_{SFD}$, and the UCA method are presented in Table 1. LS-TOOL$_{MFD}$ slope lengths closely coincided with the slope length estimated from the subset of DEM data. The LS calculations were also similar to the values of the field data. These results suggest that LS-TOOL$_{MFD}$ provides the best calculations for slope length and LS, i.e. best approximating the field data.

4. Discussion

The main differences between the results from LS-TOOL$_{MFD}$ and LS-TOOL$_{SFD}$ were due to the large differences between the SFD and MFD methods in the allocation of slope length: the MFD method disperses flow along several directions, but the SFD method is a nondispersive method where the direction of flow is only in the steepest direction. The frequency curves for slope length and LS are thus more smooth for LS-TOOL$_{MFD}$ than for LS-TOOL$_{SFD}$ (Fig. 7). Slope length and LS calculated by LS-TOOL$_{MFD}$ increased more gently along hillslopes because of the dispersive feature (Fig. 8d, e), and the mean slope lengths were higher than calculated with LS-TOOL$_{SFD}$. The percentages of slope length < 300 m and LS < 22 were thus higher with LS-TOOL$_{MFD}$ than LS-TOOL$_{SFD}$ (Fig. 7).

Slope length normally increases steadily along a hillside before reaching the cutoff point, so the slope length of the frequency curve was expected to change smoothly. The frequency curve for slope length was smoother and more evenly distributed with LS-TOOL$_{MFD}$ than LS-TOOL$_{SFD}$ (Fig. 7a, c), and better matched the field data.

LS-TOOL$_{MFD}$ produced smoother patterns of spatial distribution for slope length and LS than LS-TOOL$_{SFD}$, mainly because of the different algorithms for flow direction. LS-TOOL$_{MFD,}$ using the MFD algorithm, uses weighted values to reduce cell-to-cell differences. LS-TOOL$_{SFD}$, however, using the SFD algorithm, uses the steepest downslope direction to calculate slope length, so all slope length will be transferred to the next cell, thereby increasing the variances and skews of the distributions. These results agreed with those by Wolock and McCabe (1995), who compared single-flow and multiple-flow direction methods for the soil-erosion model TOPMODEL. Wilson et al. (2007) compared the hydrological performance of the flow-routing algorithms and also found that the SFD method produced more 'low flow' cells. (Orlandini

et al., 2012) also showed that the MFD method performed best at very high resolutions.

The results of the field data and LS-TOOL$_{MFD}$ were strongly correlated (Fig. 9a, b). A larger R^2 was found for LS than for slope length, perhaps because the error in calculating slope gradient did not accumulate and was only for one grid, but the error in calculating slope length accumulated from the start point along the flow path until the end of the flow path. Also, slope length is very sensitive to elevation, which determines the flow direction in LS-TOOL$_{MFD}$, so a different flow direction would have a different length.

UCA method also used MFD algorithm to evaluate LS factor, however, more bias than the other methods. By comparing Fig. 9b, d, e, we can see that the UCA method converts slope length to unit contributing area for considering the two-dimensional topography. However UCA method is not able to predict the slope cutoff point (e.g. flats) and channels. So some of the LS values from the field data were almost zero, which the UCA method could not predict. This is the main reason why UCA method has a lower R^2 than the other two methods.

Some of the results were not satisfactory despite the positive relationship between the field data and LS-TOOL$_{MFD}$. Flow convergence and divergence were not taken into account in the fieldwork; the average slope length calculated by LS-TOOL$_{MFD}$ differed slightly from that calculated from the field data at several locations in the landscape, especially those near channels.

The RMSEs in Table 1 indicate that most of the LS values calculated by LS-TOOL$_{MFD}$, LS-TOOL$_{SFD}$, and the UCA method were similar to those from the field data. The UCA method, however, yielded more biased results only at some locations where slope gradient changed abruptly, which included areas of residential development, channels, and road construction. Some of the LS values from the field data were near zero, which the UCA method could not predict (Fig. 9e), because the UCA method only obtains the accumulation area rather than the slope length.

Identifying the threshold of channel networks is one of the main difficulties in calculating slope length. Different threshold should be used for different areas. However, identifying all channel heads accurately was beyond the scope of this study. New methods, e.g. GeoNet (Sangireddy et al., 2016), should be considered for extracting channel networks in future studies.

Terraces are also known to affect slope length (Lopez-Vicente and Navas, 2009; Panagos et al., 2015). We did not attempt to address the terracing issue here, but we selected a small terraced sub-catchment in the Longquan catchment of Gansu province to test the impacts of input DEM resolution on the calculated slope length and LS factor in a previous study (Zhang et al., 2017). The input DEMs were at resolutions of 0.5 m (derived from unmanned aerial photogrammetric data for March 2015). This study showed that the effect of terraced fields on slope length was large. This also indicated that our algorithm worked well while encountering terrain changes abruptly (e.g. terrace) area in calculating slope length and LS factor.

Despite the shortcomings, RUSLE/USLE are still used widely to estimate soil erosion all over the world (Panagos et al., 2015; Yang, 2015). Panagos et al. (2015) improved UCA method with slope cutoff point considered to estimate LS factor for the whole Europe. We tried this method with slope cutoff point 0.5 was assigned (Panagos et al., 2015). The R^2 of the result increased 0.71, however was still lower than LS-TOOL$_{MFD}$. Yang (2015) used an automatic GIS procedure which is similar with LS-TOOL$_{SFD}$ to obtain LS factor map of New South Wales. Such an approach is an important step forward in accurate LS calculation for large areas, and our method are heading in the same direction but aiming a more accuracy flow direction algorithm. The CSLE, applied in China (Liu et al., 2002), uses a different algorithm for steeper slopes ($> 10^{\circ}$) to estimate the LS factor. Although, the research area contained slopes that were $> 10^{\circ}$, we focussed on a more accurate slope length, and so the RUSLE (and not the CSLE) is used in this paper. For areas that contain many slopes of $> 10^{\circ}$ slopes, the CSLE should be selected.

More field tests of the model are required for obtaining more accurate predictions of LS in convergent and divergent areas. The impact of cell size on changes in slope also requires further study. Larger scale field measurements are necessary to revise the algorithm to enable the model to produce more accurate results.

5. Conclusion

Integration of a multiple flow direction algorithm, the distance-transform error method and cutoff effect to calculate slope length and LS factor was proved useful. Evaluation of the results shows that the spatial distribution of slope lengths was found to be better representing the actual terrain as compared with LS-TOOL$_{SFD}$ methods, because the slope lengths are distributed over multiple cells instead of transferred to only one cell. The method was compared to existing methods (e.g. LS-TOOL$_{SFD}$ and UCA). We found that LS-TOOL$_{MFD}$ calculated slope length and LS more accurately than other methods when compared to field data. Moreover, the user-friendly interface of LS-TOOL$_{MFD}$ is useful in any model of soil erosion. The applicability and efficiency of the proposed LS-TOOL$_{MFD}$ algorithm may be significantly improved in the future by some new flow direction extraction methods (Shin and Paik, 2017; Zhang et al., 2017), none the less this is an important step toward conducting large area erosion evaluation, it overcomes the limitations of the UCA method, and improves the flow direction method in LS-TOOL$_{SFD}$.

Acknowledgement

The authors would like to express great appreciation to Meng Wang, Zelu Song Shangshang Yu for their hard field work. Lei Wang, Weiling Guo, Jun Li and Lanqin Guo from Institute of Soil and Water Conservation, Chinese Academy of Sciences, for providing helpful comments on an earlier draft of this manuscript. Thanks to Dr. William Blackhall for language edition. This research was supported by Major Project of National Key R & D Plan from the MOST of China [2017YFC0403203]; National Natural Science Foundation of China [41771315, 41301283, 41301507, 41371274]; Natural Science Foundation of Shaanxi Province [2016JM6038, 2015JM4142] and the Fundamental Research Funds for the Central Universities [2452015060, 2013BSJJ105]. And also partly supported by EU Horizon 2020 research and innovation programme (ISQAPER) [635750]; State Key Laboratory of Soil Erosion and Dryland Farming on the Loess Plateau [A314021402-1702]. Thanks also to the anonymous reviewers who all made valuable comments that improved our paper. Anyone who wants to use this tool can send email to the authors for application.

References

Desmet, P.J.J., Govers, G., 1996. A GIS procedure for the automated calculation of the USLE LS factor on topographically complex landscape units. J. Soil Water Conserv. 51, 427–433.

Dunn, M., Hickey, R., 1998. The effect of slope algorithms on slope estimates within a GIS. Cartography 27 (1), 9–15.

Feng, T., Chen, H., Polyakov, V.O., Wang, K., Zhang, X., Zhang, W., 2016. Soil erosion rates in two karst peak-cluster depression basins of northwest Guangxi, China: comparison of the RUSLE model with 137Cs measurements. Geomorphology 253, 217–224.

Galdino, S., Sano, E.E., Andrade, R.G., Grego, C.R., Nogueira, S.F., Bragantini, C., Flosi, A.H.G., 2016. Large-scale modeling of soil erosion with RUSLE for conservationist planning of degraded cultivated Brazilian pastures. Land Degrad. Dev. 27 (3), 773–784.

Griffin, M.L., Beasley, D.B., Fletcher, J.J., Foster, G.R., 1988. Estimating soil loss on topographically nonuniform field and farm units. J. Soil Water Conserv. 43 (4), 326–331.

Hickey, R., 2000. Slope angle and slope length solutions for GIS. Cartography 29 (1), 1–8.

Jabbar, M., 2003. Application of GIS to estimate soil erosion using RUSLE. Geo-Spatial Inf. Sci. 6 (1), 34–37.

Ligonja, P.J., Shrestha, R.P., 2015. Soil erosion assessment in kondoa eroded area in Tanzania using universal soil loss equation, geographic information systems and socioeconomic approach. Land Degrad. Dev. 26 (4), 367–379.

Liu, B.Y., Zhang, K.L., Xie, Y., 2002. An Empirical Soil Loss Equation, Process of 12th International Soil Conservation Organization Conference. Tsinghua Press, Beijing, pp. 143–149.
Lopez-Vicente, M., Navas, A., 2009. Predicting soil erosion with RUSLE in Mediterranean agricultural systems at catchment scale. Soil Sci. 174 (5), 272–282.
McCool, D.K., Foster, G.R., Weesies, G.A., 1997. Slope Length and Steepness Factors (LS). 703 United States Department of Agriculture, Agricultural Research Service (USDA-ARS) Handbook.
Moore, I.D., Burch, G.J., 1986a. Physical basis of the length-slope factor in the universal soil loss equation. Soil Sci. Soc. Am. J. 50 (5), 1294–1298.
Moore, I.D., Burch, G.J., 1986b. Modelling erosion and deposition: topographic effects. Trans. ASAE 29 (6), 1624–1630.
Moore, I.D., Wilson, J.P., 1992. Length-slope factors for the revised universal soil loss equation: simplified method of estimation. J. Soil Water Conserv. 47 (5), 423–428.
O'Callaghan, J.F., Mark, D.M., 1984. The extraction of drainage networks from digital elevation data. Comp. Vision Graph. Image Process. 28 (3), 323–344.
Orlandini, S., Moretti, G., Corticelli, M.A., Santangelo, P.E., Capra, A., Rivola, R., Albertson, J.D., 2012. Evaluation of flow direction methods against field observations of overland flow dispersion. Water Resour. Res. 48, 13.
Orlandini, S., Moretti, G., Gavioli, A., 2014. Analytical basis for determining slope lines in grid digital elevation models. Water Resour. Res. 50 (1), 526–539.
Panagos, P., Borrelli, P., Meusburger, K., 2015. A new European slope length and steepness factor (LS-factor) for modeling soil erosion by water. Geosciences 5 (2), 117–126.
da Paz, A.R., Collischonn, W., Riss, A., Mendes, C.A.B., 2008. Errors in river lengths derived from raster digital elevation models. Comput. Geosci. 34 (11), 1584–1596.
Quinn, P., Beven, K., Chevallier, P., Planchon, O., 1991. The prediction of hillslope flow paths for distributed hydrological modelling using digital terrain models. Hydrol. Process. 5 (1), 59–79.
Renard, K.G., Foster, G.R., Weesies, G.A., Porter, J.P., 1991. RUSLE: revised universal soil loss equation. J. Soil Water Conserv. 46 (1), 30–33.
Renard, K.G., Foster, G.R., Weesies, G.A., McCool, D.K., Yoder, D.C., 1997. Predicting soil erosion by water: a guide to conservation planning with the Revised Universal Soil Loss Equation (RUSLE). In: Agriculture Handbook.
Rodriguez, J.L.G., Suarez, M.C.G., 2012. Methodology for estimating the topographic factor LS of RUSLE3D and USPED using GIS. Geomorphology 175–176 (0), 98–106.
Sangireddy, H., Stark, C.P., Kladzyk, A., Passalacqua, P., 2016. GeoNet: an open source software for the automatic and objective extraction of channel heads, channel network, and channel morphology from high resolution topography data. Environ. Model. Softw. 83, 58–73.
Shin, S., Paik, K., 2017. An improved method for single flow direction calculation in grid digital elevation models. Hydrol. Process (n/a-n/a).
de Smith, M.J., 2004. Distance transforms as a new tool in spatial analysis, urban planning, and GIS. Environ. Plan. B-Plan. Des. 31 (1), 85–104.
Tarboton, D.G., Bras, R.L., Rodriguez-Iturbe, I., 1991. On the extraction of channel networks from digital elevation data. Hydrol. Process. 5, 81–100.
Van Remortel, R.D., Hamilton, M.E., Hickey, R.J., 2001. Estimating the LS factor for RUSLE through iterative slope length processing of digital elevation data. Cartography 30 (1), 27–35.
Van Remortel, R.D., Maichle, R.W., Hickey, R.J., 2004. Computing the LS factor for the Revised Universal Soil Loss Equation through array-based slope processing of digital elevation data using a C + + executable. Comput. Geosci. 30 (9), 1043–1053.
Wilson, J.P., 1986. Estimating the topographic factor in the universal soil loss equation for watersheds. J. Soil Water Conserv. 41 (3), 179–184.
Wilson, J.P., Lam, C.S., Deng, Y., 2007. Comparison of the performance of flow-routing algorithms used in GIS-based hydrologic analysis. Hydrol. Process. 21 (8), 1026–1044.
Winchell, M.F., Jackson, S.H., Wadley, A.M., Srinivasan, R., 2008. Extension and validation of a geographic information system-based method for calculating the revised universal soil loss equation length-slop factor for erosion risk assessments in large watersheds. J. Soil Water Conserv. 63 (3), 105–111.
Wischmeier, W.H., Smith, D.D., 1978. Predicting rainfall erosion losses: a guide to conservation planning with Universal Soil Loss Equation (USLE). In: Agriculture Handbook. Department of Agriculture, Washington, D C (No 703).
Wolock, D.M., McCabe Jr., G.J., 1995. Comparison of single and multiple flow direction algorithms for computing topographic parameters in TOPMODEL. Water Resour. Res. 31 (5), 1315–1324.
Wood, J.D., 1996. The Geomorphological Characterisation of Digital Elevation Models. University of Leicester, UK.
Yang, X.H., 2015. Digital mapping of RUSLE slope length and steepness factor across New South Wales, Australia. Soil Res. 53 (2), 216–225.
Yang, Q.K., McVicar, T.R., Van Niel, T.G., Hutchinsond, M.F., LingTao, L., XiaoPing, Z., 2007. Improving terrain representation of a digital elevation model by reducing source data errors and optimising interpolation algorithm parameters: an example in the Loess Plateau. China Int. J. Appl. Earth Obs. Geoinformation (JAG) 9 (3), 235–246.
Yang, Q., Guo, M., Li, Z., Wang, C., 2013. Extraction and analysis of China soil erosion topographic factor. Soil Water Convers. China (10), 17–21 (In Chinese).
Yao, Z.H., Yang, Q.K., Xie, H.X., Li, R., 2012. Application of Chinese Soil Loss Equation (CSLE) to analyze the spatial and temporal variations in soil erosion on the Loess Plateau of China. J. Food Agric. Environ. 10 (3–4), 1285–1293.
Zhang, H., Yang, Q., Li, R., Liu, Q., Moore, D., He, P., Ritsema, C.J., Geissen, V., 2013. Extension of a GIS procedure for calculating the RUSLE equation LS factor. Comput. Geosci. 52 (0), 177–188.
Zhang, H., Yao, Z., Yang, Q., Li, S., Baartman, J.E.M., Gai, L., Yao, M., Yang, X., Ritsema, C.J., Geissen, V., 2017. An integrated algorithm to evaluate flow direction and flow accumulation in flat regions of hydrologically corrected DEMs. Catena 151, 174–181.
Zhou, Q.M., Liu, X.J., 2004. Error analysis on grid-based slope and aspect algorithms. Photogramm. Eng. Remote. Sens. 70 (8), 957–962.